0888-8809/06/$15.00/0
Printed in U.S.A.

Molecular Endocrinology 20(5):1164–1176

doi: 10.1210/me.2005-0361

Twenty-Four-Hour Rhythmic Gene Expression in the Rhesus Macaque Adrenal Gland

Dario R. Lemos, Jodi L. Downs, and Henryk F. Urbanski

Division of Neuroscience, Oregon National Primate Research Center, Beaverton, Oregon 97006

The suprachiasmatic nucleus plays a key role in the circadian secretion of adrenocortical hormones. However, there is evidence from mouse studies that components of the circadian clock are also expressed within the adrenal gland itself. In the present study we performed genome-wide expression profiling to determine whether the adrenal gland of rhesus monkeys shows temporal gene expression across a 24-h period. We identified 322 transcripts with rhythmic patterns of expression and found that the phase distribution of cycling transcripts varied across the day, with more genes showing activation during the night. We classified the transcripts by their function and clustered them according to their participation in common biochemical pathways: 1) catecholamine synthesis and reuptake; 2) cholesterol cleavage and dehydroepiandrosterone sulfate synthesis; 3) protein synthesis and turnover; and 4) the circadian clock mechanism. In an additional experiment, we assessed the expression of various clock genes at two time points, 12 h apart. We found that expression of *Bmal1* and *Cry1* was higher at 1300 h, or *zeitgeber* time 6, whereas expression of *Per1* was higher at 0100 h (*zeitgeber* time 18). Expression levels of *Rev-erbα* were higher at 0100 h than at 1300 h ($P < 0.05$), and immunohistochemistry revealed a strong expression of this transcription factor specifically in chromaffin cells of the adrenal medulla. Taken together, the data indicate that the primate adrenal gland shows rhythmic expression of genes associated with cell biology and synthesis of steroids and catecholamines. Moreover, they strongly imply the existence of an intrinsic circadian clock. (*Molecular Endocrinology* 20: 1164–1176, 2006)

MAJOR PHYSIOLOGICAL functions, such as metabolism, thermoregulation, reproduction, and the response to stress, are regulated by hormones, many of which display a diurnal pattern of secretion. Within the human endocrine system, the adrenal gland is especially prominent because of its robust circadian release of cortisol and dehydroepiandrosterone. To a lesser extent, the secretion of catecholamines also has a diurnal rhythm. Plasma cortisol and dehydroepiandrosterone sulfate (DHEAS) concentrations show a peak in the morning, whereas plasma catecholamines show a peak in the middle of the day (1–5). The circadian mechanisms regulating adrenal hormone secretion have been studied widely in rodents, and the results show that a functional connection exists between the suprachiasmatic nucleus (SCN) and the adrenal cortex (6, 7). In rats, the SCN appears to communicate with the adrenal glands via at least two pathways: a direct one involving the autonomic nervous system, and an indirect one that involves the release of ACTH from the pituitary gland (8, 9). Although the SCN harbors a master circadian oscillator that synchronizes and sustains circadian rhythms in behavior and physiology, genetic components of the circadian clock mechanism are also expressed in various peripheral tissues (10–13). These observations raise the possibility that circadian physiology is ultimately controlled by a network of coordinated circadian oscillators, rather than by a single master clock (14).

At the intracellular level, the molecular clock mechanism appears to be highly conserved, involving coupled transcriptional/translational feedback loops that are driven by both positive and negative genetic components. In mammals, the positive components comprise the transcriptional activators CLOCK and BMAL1, which dimerize and bind to E boxes in the promoter regions of various genes, including the negative components. The negative components include the Period proteins (PER1, PER2, PER3) and Cryptochrome proteins (CRY1, CRY2), which in turn inhibit the synthesis of the Clock/Bmal1 complex, and then generate a circadian rhythm in their own transcription (15–18).

Gene microarray data from mouse SCN, liver, and heart have shown that circadian transcriptional mechanisms temporally regulate biochemical pathways within each tissue, by driving the circadian expression of specific sets of genes (19–22). Overall, these studies demonstrate that many genes involved in tissue-specific pathways, as well as general cellular path-

First Published Online January 26, 2006

Abbreviations: DAB, 3,3′-Diaminobenzidine tetrachloride; DHEAS, dehydroepiandrosterone sulfate; F, forward; KPBS, potassium PBS; qRT-PCR, quantitative RT-PCR; R, reverse; SCN, suprachiasmatic nucleus; sqRT-PCR, semiquantitative RT-PCR; TH, tyrosine hydroxylase; ZT0, *zeitgeber* time zero.

***Molecular Endocrinology* is published monthly by The Endocrine Society (http://www.endo-society.org), the foremost professional society serving the endocrine community.**

ways, accumulate in a circadian manner and in many cases appear to be controlled by a circadian clock. A deeper understanding of the circadian expression of genes associated with synthesis of hormones and neurotransmitter receptors, as well as genes involved in cell cycle and tumor suppression, has enormous biomedical potential (23, 24); however, this subject has only recently begun to be explored in primates (25–27). In view of the strong rhythmic profile of many of the adrenal functions and the circadian expression of *Period* genes in the adrenal gland of mice (28, 29), our goal was to test the hypothesis that circadian transcriptional mechanisms regulate specific pathways within the primate adrenal gland. We searched for rhythmic patterns of gene expression in the adrenal gland of the rhesus macaque by analyzing the transcriptome across a 24-h period. We found that key genes, including those involved in rate-limiting steps in the synthesis of catecholamines, cleavage of cholesterol, synthesis of DHEAS, and protein synthesis and turnover oscillated with a 24-h rhythm. Moreover, our results strongly imply the existence of an intrinsic molecular clock mechanism within this organ.

RESULTS

Diurnal Variations in Adrenal Plasma Hormone Levels

Six female rhesus macaques were maintained under a 12-h light, 12-h dark photoperiod, lights on at 0700 h [*zeitgeber* time zero (ZT0)], and their activity-rest cycles were continuously monitored (Fig. 1). To establish the temporal pattern of adrenocortical secretion in these animals, plasma concentrations of cortisol and DHEAS were measured in remotely collected blood samples. Both adrenal steroids showed a circadian rhythm across 24 h, with the levels rising during the night and peaks occurring around 0800 h (ZT1), at the time of morning activity onset (Fig. 1).

Plasma concentrations of epinephrine were measured in a group of seven middle-aged male rhesus macaques, at two time points 12 h apart, maintained under a 12-h light, 12-h dark photoperiod, lights on at 0700 h (ZT0). The mean values $\pm$ SEM at 1300 h (ZT6) and at 0100 h (ZT18) were 36 $\pm$ 6.8 and 18 $\pm$ 4.4 pg/ml, respectively ($P < 0.01$, paired Student's *t* test) (Rasmussen, D., and H. F. Urbanski, unpublished observations).

Phase Analysis of Microarray Data

The animals were killed at six time points across a 24-h period, with 4-h intervals: 0700 h (ZT0), 1100 h (ZT4), 1500 h (ZT8), 1900 h (ZT12), 2300 h (ZT16), and 0300 h (ZT20). Total RNA was isolated from the whole left adrenal gland and used to perform hybridizations on Affymetrix human HG_U133A gene microarray platforms and PCR experiments. The Affymetrix MAS 5.0 analysis software was used to analyze scanner image files and thereby generate raw data. After two consecutive filtering iterations, comprising a filter for significant amplitude and a filter for rhythmicity with a period of 24 h, both intended to identify robust oscillatory genes, 322 transcripts were identified. These transcripts were then organized by hierarchical clustering, using cosine correlation for distance measure, which yielded a temporal profile of rhythmic gene expression in the adrenal gland. The oscillation curves showed a variety of phases and amplitudes, with peaks of expression distributed throughout the 24-h cycle (Fig. 2A; and supplemental Table 1 published on The Endocrine Society's Journals Online web site at http://mend.endojournals.org).

Next, the phase distributions were analyzed by clustering the transcripts using a *k*-means method; the expression profiles were grouped into six clusters, each corresponding to one of the six sampling times (Fig. 2B). Interestingly, the phase distributions of the various genes were not homogeneous: 70 transcripts peaked at 0300 h (ZT20), 75 transcripts at 0700 h (ZT0), 41 transcripts at 1100 h (ZT4), 30 transcripts at 1500 h (ZT8), 44 transcripts at 1900 h (ZT12), and 62 transcripts at 2300 h (ZT16) (Fig. 2C). Taken together these data indicate that the number of cycling transcripts increased during the night, starting at around 1900 h (ZT12), and reached a maximum at 0700 h (ZT0), when the lights came on in the morning (Fig. 2C). The number of cycling transcripts reduced abruptly between 0700 h (ZT0) and 1100 h (ZT4), and reached a minimum at 1500 h (ZT8).

Functional Categories and Clusters

A gene annotation tool was used to obtain gene abbreviations and descriptions and to cluster the 322 transcripts into common biochemical pathways. This enabled us to work with a physiological view of the transcriptome and to determine at which stages each of those pathways was temporally regulated. Four main clusters emerged from the analysis, and included genes involved in: 1) catecholamine synthesis and reuptake; 2) cholesterol cleavage and DHEAS synthesis; 3) protein synthesis and turnover; and 4) the circadian clock mechanism.

Transcripts Involved in Catecholamine Synthesis and Reuptake. Rhythmic expression of genes involved in catecholamine synthesis and reuptake included tyrosine hydroxylase (*TH*), phenylethanolamine *N*-methyl transferase (*PNMT*), and the norepinephrine transporter 2 (*Slc6A2*) (Fig. 3A). *TH* and *PNMT* expression peaks occurred at approximately 0700 h (ZT0), whereas the expression peak of *Slc6A2*, detected by two different probe sets, occurred at approximately 1900 h (ZT12). The expression pattern of *TH* was validated by Taqman quantitative RT-PCR (Taqman qRT-PCR) (Fig. 3A), whereas the expression patterns of *PNMT* and *Slc6A2* were validated by semiquantitative RT-PCR (sqRT-PCR) (Fig. 3B). As an internal control

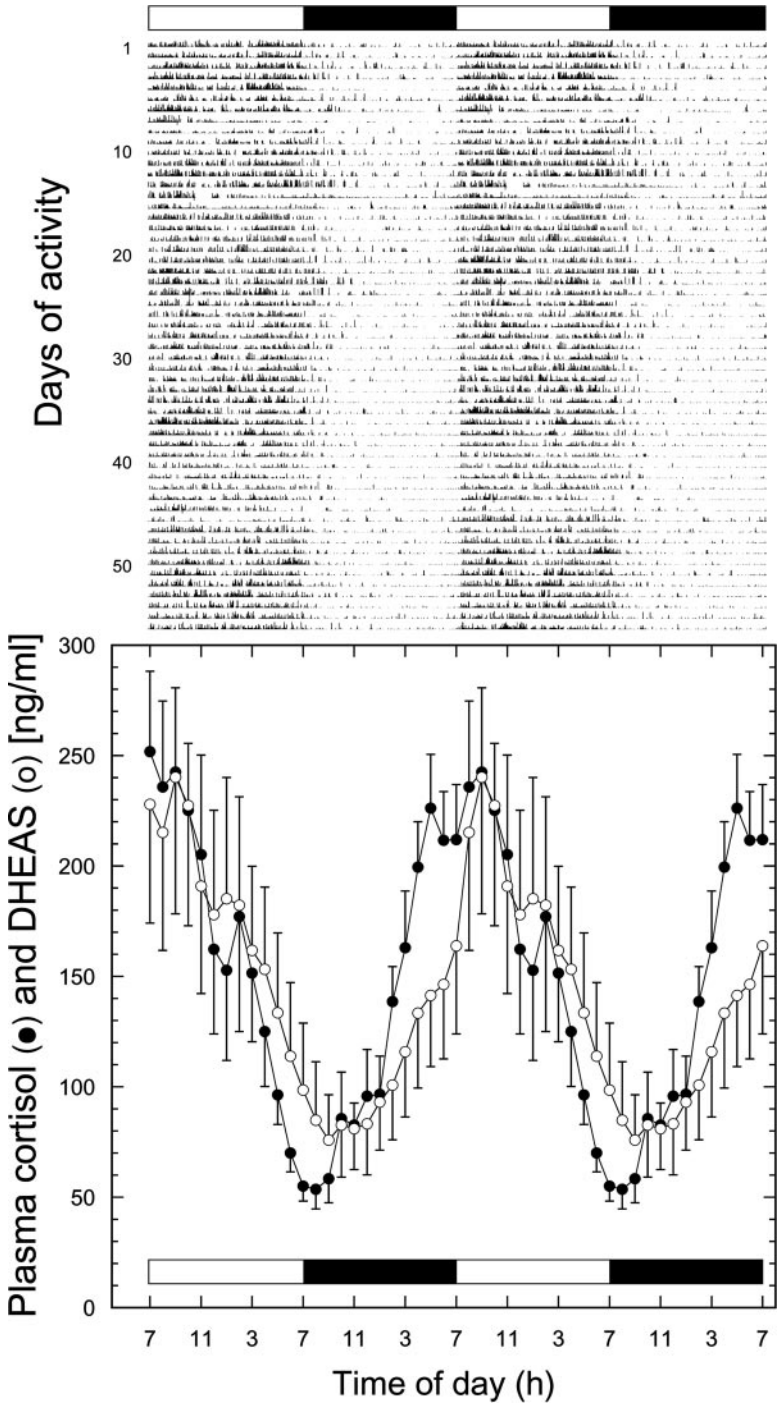

Fig. 1. Diurnal Rhythms in Locomotor Activity and Adrenocortical Hormone Secretion in Female Rhesus Macaques

Upper panel, Locomotor activity patterns (24 h) from a representative animal. *Lower panel*, Mean (± SEM) 24-h plasma concentration of cortisol and DHEAS from six animals; the hourly blood samples were collected using a remote swivel/tether-based sampling system (5). All the data are double plotted, to facilitate viewing of the 24-h rhythms. The *white and black bars* represent day and nighttime, respectively. Note the coincidence of the hormone peaks at the time of activity onset in the morning.

for all the clusters, *β-actin* was assessed by sqRT-PCR (see Fig. 6B).

Transcripts Involved in Cholesterol Cleavage and DHEAS Synthesis. The cluster of genes involved in cholesterol cleavage and synthesis of DHEAS included: cholesterol side chain cleavage (*Cyp11A1*), steroid 17-α-hydroxylase (*Cyp17A*), cytochrome b-5 (*Cyb5*), and dehydroepiandrosterone sulfotransferase (*SULT2A1*)

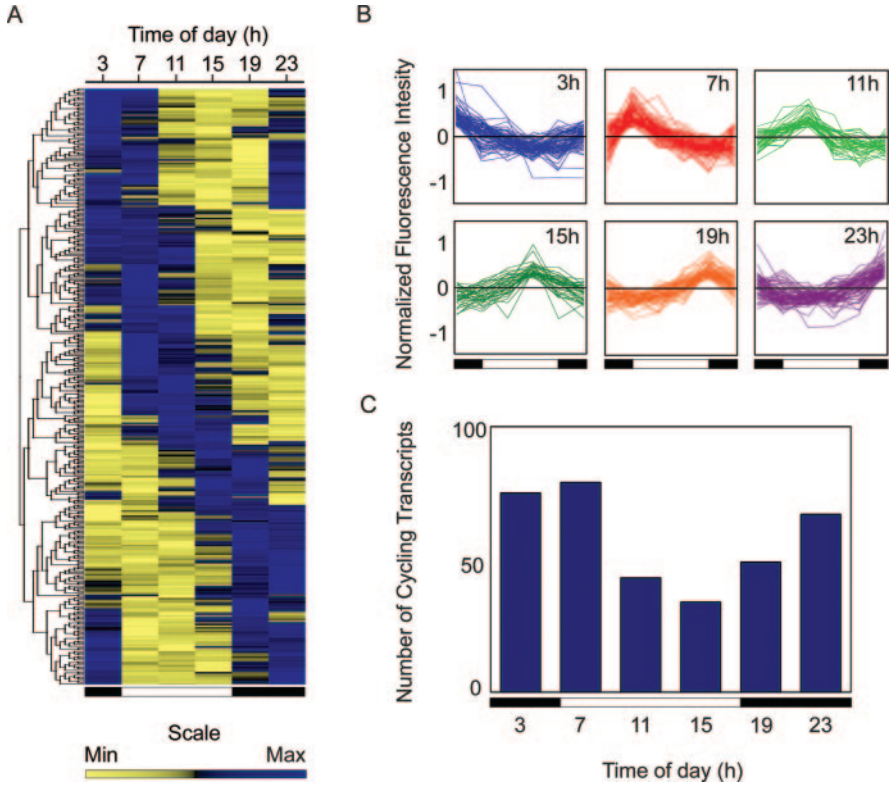

Fig. 2. Temporal Gene Expression Profiles in the Rhesus Macaque Adrenal Gland

A, Hierarchical clustering of the 322 oscillating transcripts. Each *column* represents a time point, and each *row* represents a gene. Relationships between genes are depicted as a *tree*, with *branch length* reflecting the degree of similarity in time courses between the genes. For a complete list of genes, symbols, and associated expression values, see supplemental data. B, Gene expression profiles showing different phases across 24 h; the data have been normalized such that the medial signal intensity for each gene across all time points is 0. C, Distribution of cycling transcripts across 24 h. In all *panels*, the *white and black bars* represent day and nighttime, respectively. Min, Minimum; Max, maximum.

(Fig. 4A). The four transcripts showed a rhythmic pattern of expression with peaks between 1900 h (ZT12) and 2300 h (ZT16). Expression profiles obtained by sqRT-PCR for *Cyp11A1* and *Cyp17A* were consistent with the results from the gene microarrays (Fig. 4B).

Transcripts Involved in Protein Synthesis and Turnover. The genes represented in the protein turnover cluster are involved in various stages of protein synthesis, processing, secretion, and degradation (Fig. 5A). The cluster comprised six subsets: 1) subset of ribosomal proteins: ribosomal protein S7 (*Rps7*), ribosomal protein L15 (*Rpl15*), ribosomal protein L13a (*Rpl13a*), ribosomal protein L4 (*Rpl4*), ribosomal protein L39 (*Rpl39*) (Fig. 5B); 2) subset of translation initiation factors: eukaryotic translation initiation factor 3, subunit 10 θ (*Eif3S10*), eukaryotic translation initiation factor 3, subunit 6 (*Eif3S6*), eukaryotic translation initiation factor 3, subunit 5 ϵ (*Eif3S5*), translation factor sui1 homolog (*Gc20*); 3) subset of proteins involved in folding: *DnaJA1*, tetratricopeptide repeat domain 2 (*Ttc2*), heat shock 70-kDa protein 8 (*HspA8*), heat shock 105 kDa/110 kDa protein B (*Hsp105B*) (Fig. 5B); 4) subset of posttranslational modification enzymes: UDP-*N*-acetyl-α-D-galactosamine:polypeptide *N*-acetylgalactosaminyltransferase 4 (*Galnt4*), the O-linked *N*-acetylglucosamine (*GlcNAc*) transferase (*Ogt*), dolichyl-diphosphooligosaccharide-protein glycosyltransferase (*Ddost*); 5) subset of proteins involved in endoplasmic reticulum-Golgi transport: Golgi SNAP receptor complex member 2 (*GosR2*), coatomer protein complex, subunit α (*Copa*), vacuolar protein sorting 35 (*Vps35*), coated vesicle membrane protein (*Rnp24*), sorting nexin 4 (*Snx4*); 6) subset of proteins involved in ubiquitination: ubiquitin-specific protease 13 (*Usp13*), ubiquitin-specific protease 33 (*Usp33*), ubiquitin protein ligase E3A (*Ube3A*), tetratricopeptide repeat domain 3 (*Ttc3*) and proteasome components: proteasome 26S subunit 6 (*Psmc6*), proteasome activator subunit 2 (*Psme2*). Overall expression of this cluster was up-regulated between 0700 h (ZT0) and 1100 h (ZT4), and expression of the transcripts within each subset peaked with tight coordination with the exception of *Usp13* and *Galnt4* (Fig. 5A). The expression profiles for *Rps7*, *Rpl13a*, and *Rnp24* were validated by sqRT-PCR.

Transcripts Involved in the Circadian Clock Mechanism. Analysis of the fourth main cluster displayed the rhythmic expression of the clock transcripts *Per1*, *Per2*, *Bmal1*, *Cry1*, and *Rev-erb*α. Expression of the transcriptional repressors *Per1* and *Per2* peaked at

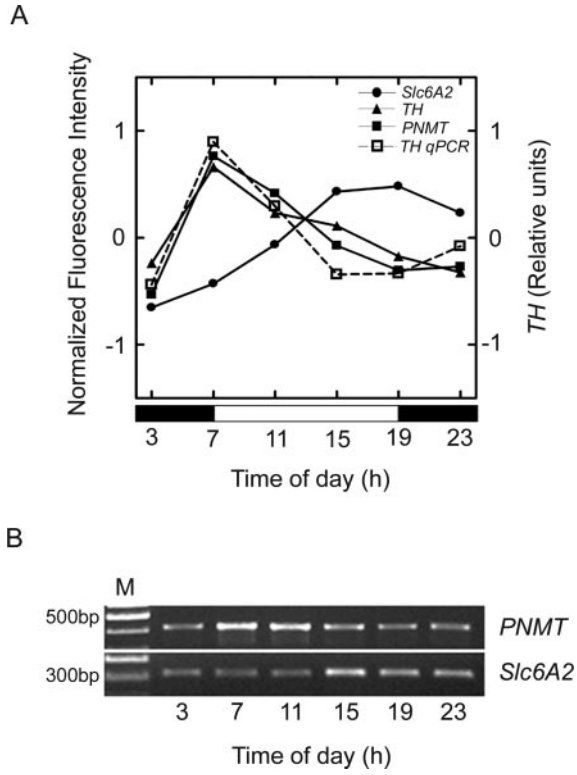

Fig. 3. Temporal Synchronization of Transcripts Associated with Catecholamine Synthesis in the Rhesus Macaque Adrenal Gland

A, *Right ordinate*, 24-h microarray profiles. *Left ordinate*, expression of *TH* relative to *β-actin*, measured by Taqman qRT-PCR; the data have been normalized such that the medial signal intensity for each gene across all time points is 0. The *white and black bar* represents day and nighttime, respectively. B, sqRT-PCR expression profiles for *PNMT* and *Slc6A.* M, Molecular weight marker.

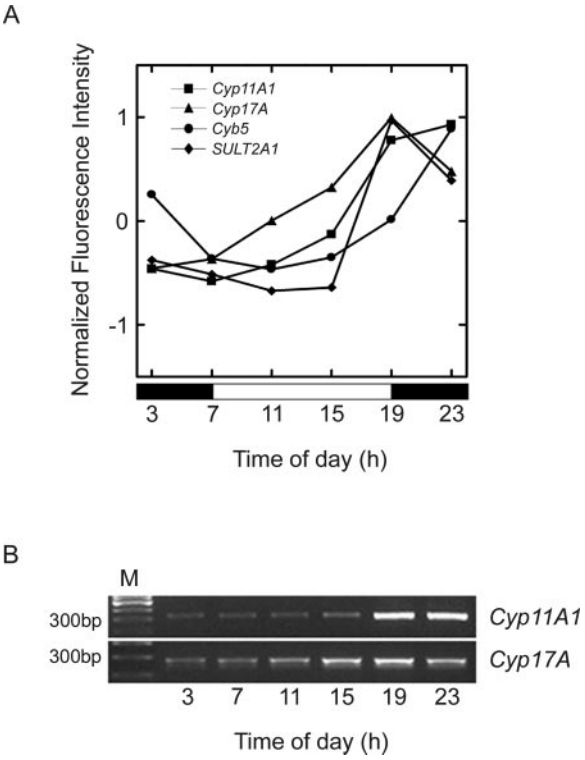

Fig. 4. Temporal Synchronization of Transcripts Associated with DHEAS Synthesis in the Rhesus Macaque Adrenal Gland

A, Microarray profiles (24 h); the data have been normalized such that the medial signal intensity for each gene across all time points is 0. The *white and black bar* represents day and nighttime, respectively. B, sqRT-PCR expression profiles for *Cyp11A1* and *Cyp17A*. M, Molecular weight marker.

approximately 0700 h (ZT0), whereas *Bmal1*, a transcriptional activator, peaked at approximately 1900 h (ZT12). The peak of expression of *Cry1* occurred at 1100 h (ZT8), 8 h after the peaks of *Per1* and *Per2* (Fig. 5A, *upper panel*), whereas the peak of *Rev-erbα* occurred at approximately 0300 h (ZT20) (Fig. 6A, *lower panel*). Although *Clock* mRNA was detected, the profile of this transcript failed to meet our statistical criteria for rhythmic expression (Fig. 6A). Rhythmic expression of core-clock genes was confirmed by the results of Taqman qRT-PCR for *Rev-erbα* (Fig. 6A, *lower panel*) and sqRT-PCR for *Per1*, *Per2*, *Bmal1*, and *Cry1* (Fig. 6B).

Expression of Core-Clock Genes at 0100 h (ZT18) *vs.* 1300 h (ZT6)

In a separate experiment, involving a different group of six adult females, we used an alternative approach and measured in triplicate the expression of clock genes in the adrenal gland, at two time points 12 h apart. The animals were maintained in a 12-h light, 12-h dark lighting regimen with lights on at 0700 h (ZT0). Three of the animals were killed at 0100 h (ZT18) and three at 1300 h (ZT6). sqRT-PCR was used to assess the expression of *Per1*, *Cry1*, and *Bmal1*, in the adrenal glands. We found that *Per1* mRNA was elevated at 0100 h (ZT18), whereas *Bmal1* and *Cry1* mRNA levels were elevated at 1300 h (ZT6) (Fig. 7A). Taqman qRT-PCR analysis of *Rev-erbα* showed significantly higher levels of expression at 0100 h (ZT18), compared with 1300 h (ZT6) (Fig. 7B).

REV-ERBα Oscillation within Chromaffin Cells of the Primate Adrenal Gland

To investigate the spatiotemporal profile of a circadian clock protein within the monkey adrenal gland, we performed immunohistochemistry on fixed monkey adrenal sections, using an antibody against the orphan nuclear receptor REV-ERBα. The nuclear staining for REV-ERBα was highly localized in the adrenal medulla (Fig. 8A), specifically within chromaffin cells, where coexpression of REV-ERBα and tyrosine hydroxylase (TH) was observed (Fig. 8B). Furthermore, the intensity of the nuclear staining changed qualitatively across

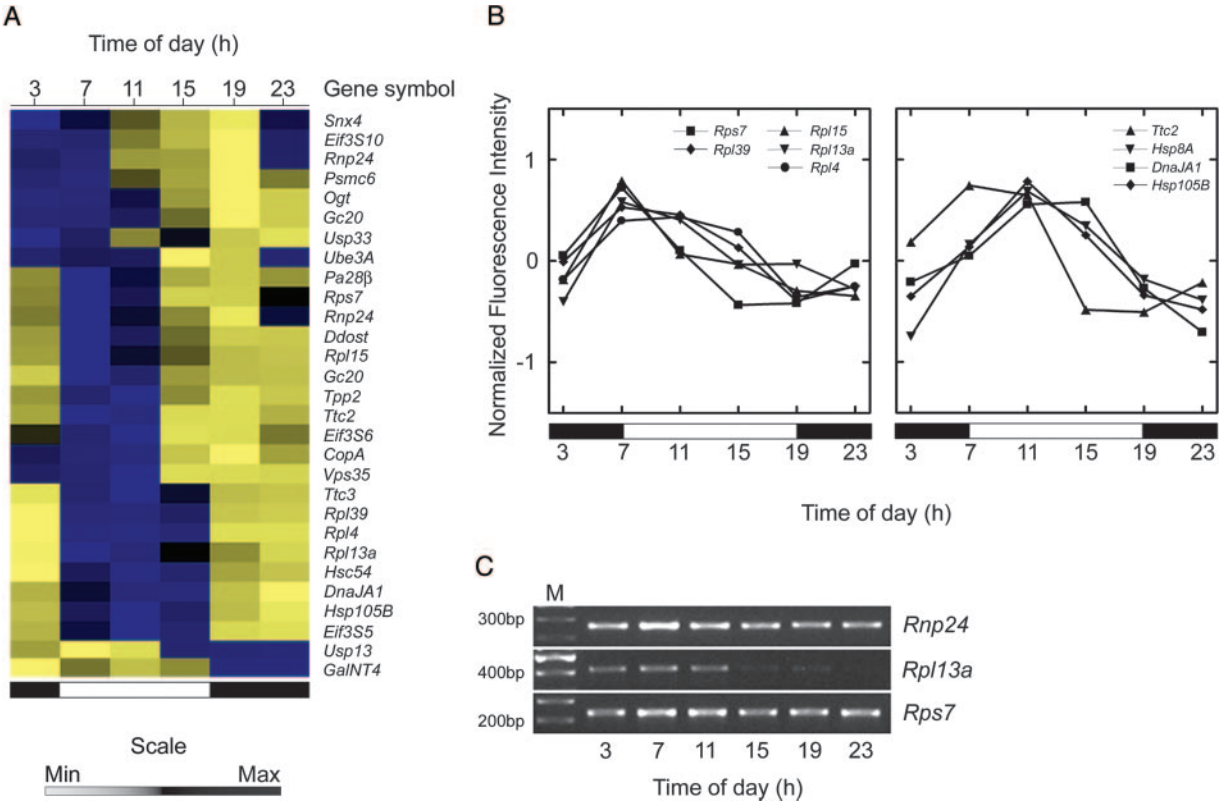

Fig. 5. Temporal Synchronization of Transcripts Associated with Protein Synthesis and Turnover in the Rhesus Macaque Adrenal Gland

A, Hierarchical clustering of genes involved in protein synthesis, processing, secretion, and degradation. Each *column* represents a time point, and each *row* represents a gene. B, Microarray profiles (24 h) of genes encoding ribosomal proteins and chaperones; the data have been normalized such that the medial signal intensity for each gene across all time points is 0. C, sqRT-PCR expression profiles for ribosomal components. M, Molecular weight marker. *White and black bars* represent day and nighttime, respectively. Min, Minimum; Max, maximum.

the 24-h day (Fig. 8C); it was particularly weak during the day and increased in intensity during the night, reaching a maximum when lights came on, at 0700 h (ZT0) *(i.e*. 4 h after the transcriptional peak). The staining was nondetectable in the adrenal cortex at any of the time points examined (supplemental Fig. 1 published on The Endocrine Society's Journals Online web site at http://mend.endojournals.org).

DISCUSSION

In the present study, we found that rhythmic hormone secretion and gene expression occur in the adrenal gland of the rhesus monkey. Like humans, rhesus monkeys are more active during the day and show a consolidated pattern of rest during the night (Fig. 1). We found that secretion of cortisol, as well as DHEAS, two steroids synthesized in the adrenal cortex, had a diurnal pattern (Fig. 1). In males, levels of plasma epinephrine, which is mainly of adrenal medulla origin, showed a diurnal pattern, when levels at 0100 h (ZT18) and 1300 h (ZT6) were compared. Taken together, these results support the view that the adrenal gland of primates, like that of rodents (30–32), is regulated by circadian mechanisms.

Our microarray data revealed the existence of oscillatory patterns of gene expression in the monkey adrenal gland. However, there are some caveats. The adrenal gland is composed of two main regions, the cortex and the medulla, which lie in very close apposition. Moreover, chromaffin cells from the medulla frequently invaginate, or migrate, into the cortex, and conversely, small clusters of cortical cells are often found in the medulla (33–35). Therefore, gross dissection of the gland and region-specific gene expression analysis may result in erroneous conclusions. Consequently, we chose to use the entire adrenal gland for our microarray analysis, even though this may have led to some loss of sensitivity, due to normalization of each probe set's intensity to an average intensity value. Also, it is possible that some genes oscillate in one region, but not in the other, or the same genes may have different phases of expression in different regions of the gland, resulting in a net cancellation of the overall oscillation pattern. As a consequence, it is

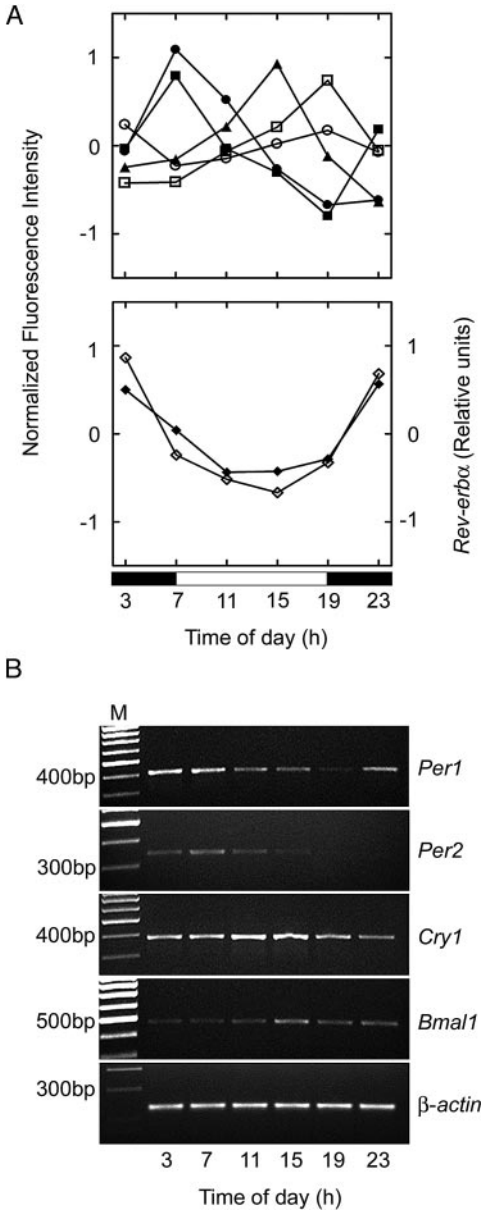

Fig. 6. Expression Profiles (24 h) of Core-Clock Genes in the Rhesus Macaque Adrenal Gland

A (*Upper panel*), Microarray profiles for *Clock*, –○–; *Per1*, –■–; *Per2*, –●–; *Cry1*, –▲–; and *Bmal1*, –□–. A (*Lower panel*), Normalized array values, –♦–; and Taqman qRT-PCR expression levels, –◇– for *Rev-erbα*. The data have been normalized such that the medial signal intensity for each gene across all time points is 0. The *white and black bar* represents day and nighttime, respectively. B, Validation of the results from the microarrays using sqRT-PCR. M, Molecular weight marker.

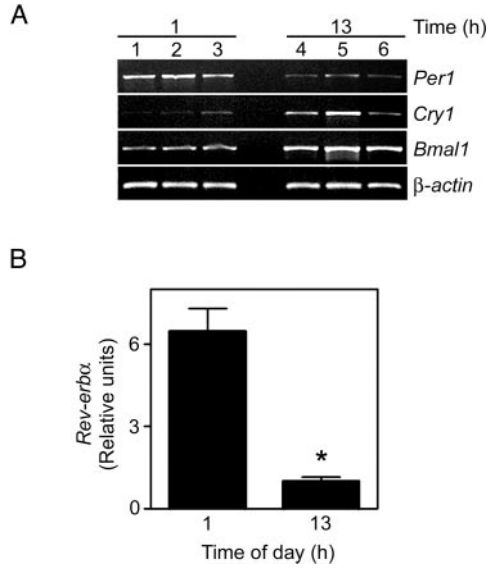

Fig. 7. Expression of Core-Clock Genes in the Rhesus Macaque Adrenal Gland at 0100 h and 1300 h, Determined in Triplicate

A, sqRT-PCR expression levels at 0100 h (lanes 1–3) and 1300 h (lanes 4–6). B, Taqman qRT-PCR expression levels for *Rev-erbα*; each *bar* represents mean data from three animals, and *vertical lines* indicate the SEM. Statistical comparisons were made by Student's *t* test (*, $P < 0.05$).

possible that in our analysis some rhythmically expressed genes fell below the detection threshold for rhythmic expression.

The analysis of phase distribution showed that the number of peaking transcripts began to increase after the lights were turned off and reached a maximum at the time when the light were turned back on in the morning, at 0700 h (ZT0). These results suggest that circadian transcriptional activating components in the rhesus macaque adrenal gland act mainly during the night phase of the 24-h day.

The analysis of gene clusters indicated that general cellular processes (*e.g*. protein synthesis), as well as pathways related to major organ-specific functions (*e.g*. catecholamines synthesis, DHEAS synthesis) are temporally coordinated at the transcriptional level. Secretion of one of the most important groups of adrenal hormones, the glucocorticoids, is regulated by humoral and neural inputs with circadian rhythms (36, 37). In the present study, the animals had strong diurnal profiles in plasma cortisol levels, with peaks early in the morning (Fig. 1). At the transcriptional level, although the mRNAs coding for CYP21A and CYP11B, the cytochromes that convert 17-hydroxyprogesterone into 11-deoxycortisol and 11-deoxycortisol into cortisol, respectively, were detected in our microarrays at each of the six time points, these transcripts failed to reach our statistical criteria for rhythmic expression, suggesting that there is no major regulation of the pathway at this level.

The four genes involved in the synthesis of DHEAS had similar patterns of expression, gradually increasing across the day and peaking with temporal proximity at the beginning of the dark phase (Fig. 9). This indicates that the pathway is transcriptionally synchronized, and differentially activated early in the night. Because we found the levels of DHEAS to peak around 0800 h (ZT1) (Fig. 1B), the time window between the

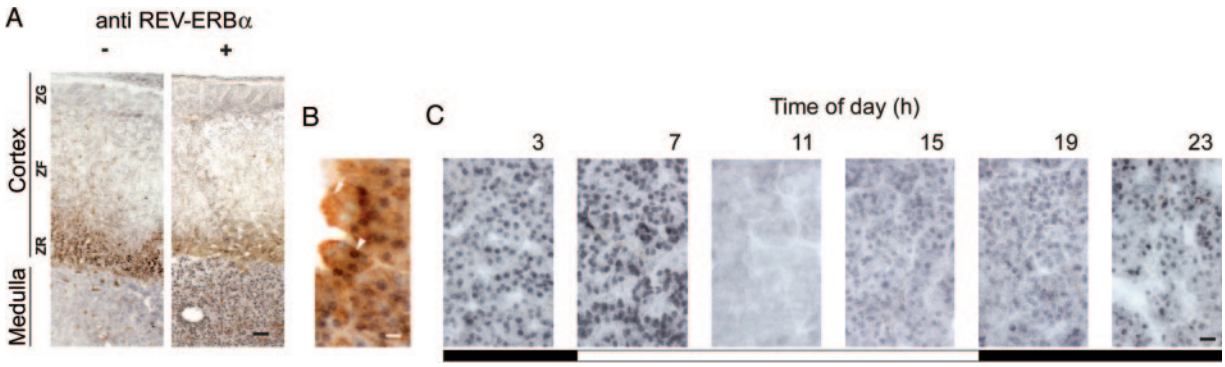

Fig. 8. Immunohistochemistry for REV-ERBα in the Rhesus Macaque Adrenal Gland

A, Photomicrographs depicting lateral sections through an adrenal gland, collected at 0700 h, and processed for immunohistochemistry using nickel-enhanced DAB as the chromogen. *Left and right panels* show the results of incubation without (negative control) or with (positive test) antibody against human REV-ERBα. *Scale bar*, 200 μm. B, Double-label immunostaining in the adrenal medulla at 0700 h, using DAB for TH (*white arrow*) and DAB/nickel for REV-ERBα (*white arrowhead*). *Scale bar*, 50 mm. C, REV-ERBα immunostaining in the adrenal medulla, showing a temporal change in intensity across 24 h. *Scale bar*, 30 μm. The *white and black bar* represents day and nighttime, respectively.

transcription of those genes and the secretion of the hormone may account for the translation of those mRNAs into functional cytochromes and enzymes for synthesis of the steroid. Expression of *Cyp11A1*, *Cyp17A*, and *SULT2A1* is activated by ACTH (38, 39), which is secreted with a circadian pattern by the pituitary (40). ACTH up-regulates the expression of *Cyp11A1* and *Cyp17A*, through cAMP-dependent mechanisms that ultimately lead to the activation of gene-specific transcription factors that bind to the promoters of *Cyp11A1*and *Cyp17A,* such as steroidogenic factor 1 and Sp1 (38, 41). Because it has been demonstrated that epinephrine activates the expression of *Cyp11A1*and *Cyp17A* (42), circadian secretion of epinephrine by chromaffin cells contacting the zona reticularis (34, 35) may also influence the rhythmic pattern of expression of these cytochromes within the cortex. Lastly, regulation of hepatic cytochrome P450s by D-site albumin promoter binding protein (DBP) and deleted in esophageal cancer 2 (DEC2), regulators of the mammalian circadian clock, has been reported (43); this suggests that *Cyp11A1*and *Cyp17A* may be regulated by a circadian clock mechanism, which is consistent with the finding that mice show a circadian expression pattern of *Cyp17A* and *Cyb5* (18, 21).

Rhythmic transcriptional regulation of catecholamine synthesis and reuptake might be of relevance for the diurnal secretion of catecholamines. In humans both the levels of epinephrine and norepinephrine in plasma peak between 1200 h and 1400 h, and decline

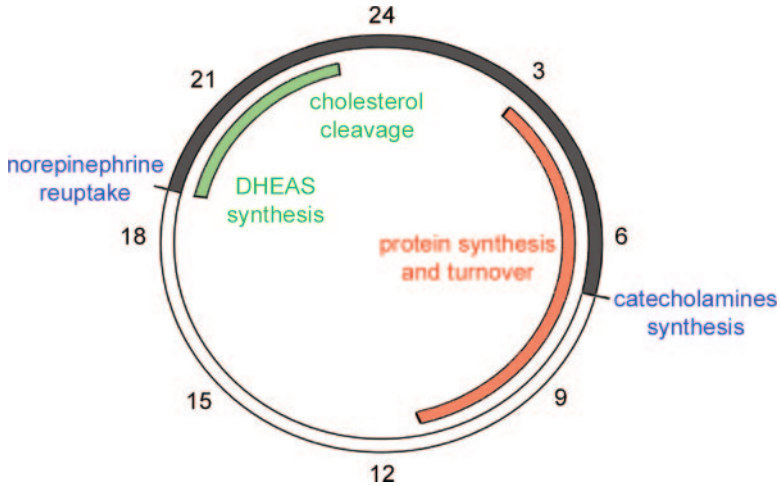

Fig. 9. Transcriptional Organization of Adrenal Biochemical Pathways across the 24-h Day

The *white and black segments of the circle* represent day and nighttime, respectively, and the *numbers around the perimeter* represent the time of day (h). The times when catecholamine synthesis and reuptake are positively regulated are indicated by *lines*. *Inner segments of the circle* represent the periods during which cholesterol cleavage and DHEAS synthesis, and protein synthesis and turnover transcripts, are positively regulated. The *colors within the circle* correspond to the names of the biochemical pathway.

during the evening (3, 4). Consistent with those previous observations, our results show that epinephrine is significantly higher at 1300 h (ZT6), compared with 0100 h (ZT18) in the rhesus macaque. Our gene expression data showed that synchronization of *TH* and *PNMT* transcription occurs at approximately 0700 h (ZT0) (Fig. 9), possibly coordinating the cytoplasmic and the intravesicular stages of the pathway during the period of synthesis of catecholamines early in the day. On the other hand, the expression peak of *Slc6A2* at approximately 1900 h (ZT12) supports the idea of an increase in the reuptake of norepinephrine and refilling of intracellular vesicles during the phase of secretion. Three important factors that affect the expression of *TH* and *PNMT* must be considered as influencing the oscillatory pattern of expression of these genes: 1) signals from the SCN that are transmitted to the adrenals through the sympathetic preganglionic cells of the intermediolateral cell column (29, 37, 44); 2) circadian secretion of glucocorticoids that regulate gene expression through the glucocorticoid receptor; and 3) transcriptional regulation by clock genes through consensus E box motifs that have been identified in the promoter region of the *TH* gene, and in the exon/intron 1 junction of the norepinephrine transporter gene (45, 46).

We found that various genes involved in protein synthesis and turnover oscillate with a rhythmic pattern in the monkey adrenal, which is consistent with previous reports of protein concentrations having circadian rhythms in the rat adrenal (47, 48). Indeed, circadian expression of genes involved in protein synthesis and turnover has been consistently reported in previous circadian microarray studies of different organisms, including *Drosophila* (49), *Arabidopsis* (50), rat-1 fibroblasts (51), and mice (18–21). Although additional studies will be necessary to elucidate the functional significance of this phenomenon, the findings suggest that, during the course of evolution, cells may have conserved a specific circadian program that organizes the pathway at different levels: ribosome, translation initiation, protein folding and sorting, glycosylation, and degradation. Moreover, they raise the question of what might happen in cells that lack functional circadian machinery (*i.e.* clock mutants), in terms of correct synthesis, gene processing and folding of new proteins, and triggering of the stress response when misfolding occurs.

Various approaches have been used to elucidate the circadian mechanisms that control diurnal adrenal function. From studies performed under free-running conditions, it is clear that adrenocortical physiology is driven by a circadian oscillator (30–32, 49, 53). For example, ablation of the SCN or destruction of its serotonergic afferents led to loss of circadian rhythm of corticosterone secretion in rats, implying a major role for the master clock in the regulation of adrenocortical function (54, 55). Moreover, a recent study showed that light, a major circadian cue, triggers the secretion of corticosterone in rats via the SCN (29). In addition to the classical pathway connecting the SCN with the adrenal through the HPA axis and the secretion of ACTH, it has also been demonstrated that the SCN drives the secretion of corticosterone through a neural pathway that involves the sympathetic innervation of the gland (29, 37). Early *in vitro* studies provided evidence that the adrenal gland might contain an intrinsic circadian oscillator (56–58). Because the adrenal is the target of multiple inputs with a circadian rhythm, the existence of a molecular clock mechanism able to organize gene expression across a 24-h day might be a way for the organ to balance its own homeostasis with the temporal demands of the body. Data from the present study demonstrate that a molecular circadian clock mechanism is likely to exist in the adrenal gland of primates. This mechanism comprises the expression of the core clock components *Clock*, *Bmal1*, *Per1*, *Per2*, *Cry1*, and *Rev-erbα*, as well as the circadian clock regulators *Dec2* and *Nfil3/E4bp4* (supplemental Table 1). The phase distribution of these transcripts was highly consistent with the mammalian clock model (59). Our 24-h transcriptome profiling experiment showed that the expression peak of the transcriptional activator *Bmal1* was approximately 12 h out of phase with the repressors *Per1* and *Per2* (Fig. 6), whereas expression of *Cry1,* similarly to what has been described in rodents (12, 21, 50), peaked approximately 8 h after *Per1* and *Per2*. In addition, we found no significant oscillation for *Clock* (Fig. 6). These results were corroborated in a second independent experiment, in which clock gene accumulation was compared between 0100 h (ZT18) and 1300 h (ZT6), two time points that were not assessed in the preceding gene microarray experiment. The results clearly confirmed the precise phase relationship for a circadian clock (Fig. 7). Moreover, it has recently been found that light up-regulates the expression of *Per1* in the adrenal gland of Per1-luc transgenic mice. Because a role for PER1 in resetting the molecular circadian clock has been proposed (60), it is plausible that light exerts a resetting effect on adrenal clock gene expression by activating PER1.

In keeping with the diurnal *vs.* nocturnal nature of monkeys and mice, respectively, a previous mouse adrenal study performed under similar photoperiodic conditions (*i.e.* 12-h light, 12-h dark conditions; lights on at 0700 h) reported that both *Per1* and *Per2* showed an expression peak at around 1630 h (ZT9.5), closer to the dark phase (28). Conversely, in the present monkey adrenal study we found that both *Per1* and *Per2* had an expression peak at the beginning of the light phase. In addition, the temporal profiles of adrenocortical secretory activity in both species are opposite: the peak of corticosterone occurs at the beginning of the dark phase in the case of mice, whereas the peak of cortisol occurs at the beginning of the light phase in the case of monkeys. Together, these results indicate that adrenal activity is temporally out of phase in diurnal mammals compared with nocturnal ones, and also that diurnal transcriptional mech-

anisms regulating gene expression within this endocrine organ have the same temporal relationship.

We found that the translated product of one of these transcripts, REV-ERBα, was expressed in the nuclei of the chromaffin cells in a circadian fashion, suggesting that this cell type harbors a molecular clock mechanism. Although we did not observe immunoreactivity for REV-ERBα in the adrenal cortex, results from mice adrenals, in which different levels of expression were found for *Per1* and *Per2* between the cortex and the medulla (28, 29), indicate that a more complete analysis of each clock component is necessary to arrive at definitive conclusions about the existence or absence of clock mechanisms in both regions. However, the *in situ* results of Bittman *et al.* (28), showing synchronous oscillation of both *Per* transcripts in the adrenal cortex and medulla of mice, suggest that if functional circadian oscillators are intrinsic to both regions they are likely to be synchronized under normal light-dark environmental conditions.

The adrenal gland plays multiple roles in human physiology, and, from a clinical perspective, abnormal functioning of specific regions of the gland may contribute to different pathologies, including obesity, diabetes, and cardiac diseases (61–63). The existence of temporal organization of gene expression, together with a circadian oscillator, within the primate adrenal introduces a new component that may help elucidate the circadian physiology of this organ.

MATERIALS AND METHODS

Animals

Six young adult female rhesus monkeys (*Macaca mulatta*; age range: 8–11 yr old) were housed in a temperature-controlled environment, under a 12-h light, 12-h dark photoperiod, lights on 0700 h (ZT0). They were fed primate chow (Purina Mills Inc., St. Louis, MO) at 0800 h (ZT1) and at 1500 h (ZT8) each day, supplemented with fresh fruit and vegetables; drinking water was available *ad libitum*. The activity-rest cycle of each animal was continuously monitored using an Actiwatch recorder (Mini Mitter Co., Inc., Sunriver, OR). The animals were cared for by the Oregon National Primate Research Center, Division of Animal Resources, in accordance with the National Institutes of Health (NIH) Guide for the Care and Use of Laboratory Animals. The research was approved by the Institutional Animal Care and Use Committee.

Hormone Assays

Blood samples were collected hourly across 24 h, using a remote swivel/tether-based sampling system (5). The assay for cortisol was performed as previously described (5, 64), utilizing a 2010 Elecsys assay instrument (Roche Diagnostics, Alameda, CA). DHEAS was assayed as previously described (5, 65), using a competitive-binding RIA kit (Diagnostic Products Corp., Los Angeles, CA).

RNA Extraction

Animals were painlessly killed (in accordance with the NIH Guide for the Care and Use of Laboratory Animals) at different times across the 24-h day. During the nighttime necropsies, the animals' eyes were covered to prevent illumination of the retina. Various tissues were collected and used in this and other unrelated studies. In all experiments, left adrenal glands were used for RNA extraction, whereas right adrenal glands were used for histology. In experiment 1 (the 24-h profile study) one adrenal gland per time point was collected. In experiment 2 (the 1-h *vs.* 13-h time point comparison study) three adrenal glands per time point were collected. The adrenals were quickly frozen in liquid N_2 and subsequently homogenized using a PowerGen rotor-stator homogenizer (Fisher Scientific, Pittsburgh, PA). Total RNA was extracted using RNeasy columns (QIAGEN, Valencia, CA); the final concentration and purity were determined by spectrophotometry, and the integrity was assessed using an Agilent 2100 Bioanalyzer (Agilent Technology, Palo Alto, CA).

Gene Microarray

Four factors dictated our use of the Affymetrix human HG_U133A gene microarray platform. First, there was no rhesus macaque gene microarray platform available at the time of this study. Second, the genetic homology between human and rhesus monkeys has been estimated to be between 92.5% and 95% (66). Third, the feasibility of using the Affymetrix human GeneChip in nonhuman primate studies has been previously demonstrated (67, 68). Fourth, application of the first filter in our microarray data analysis rigorously defined the presence of each transcript; we only selected transcripts that showed at least four Present calls of six, and this criterion ensured a reproducibility of at least 67% in the hybridization of each identified transcript.

cDNA synthesis, cRNA synthesis, hybridization, and array scanning were performed at the Affymetrix Microarray Core, Oregon Health and Science University West Campus, following the Affymetrix GeneChip Expression Analysis Technical Manual. The Matchminer software, obtained from the NCI/LMP Genomics and Bioinformatics group, was used to identify and annotate the genes represented on the microarray.

Data Analysis

Raw scanner image files were analyzed using Affymetrix MAS 5.0 absolute expression analysis software. The parameters α_1 and α_2, which set the point at which a probe set is called present (P), marginal (M), or undetectable (A), were set to 0.1 and 0.15, respectively. Comparisons were performed using global scaling, with the target intensity value set to an average intensity of 325; this allowed for the direct comparison of hybridization values from the different arrays. To extract those genes that have robust oscillatory patterns we used three statistical filters. The first filter was aimed at reducing the effect of interspecies hybridization by ensuring the reproducibility of the hybridization and the presence of that transcript; it included probe sets with at least four Present calls. To identify genes with rhythmic expression, we used an adaptation of a previously described statistical method (21, 52); we empirically tested for statistical significant cross-correlation between six time point courses of each probe set and cosine curves of defined period and phases. We used the cosine curve $\{t_i, \sqrt{2}\,Cos(2\pi\,(t_i - b)/24)\}$ with a phase b ($0 \leq b < 24$) to prepare 144 test cosine curves of 24-h periodicity, with a phase b from 0–24 h in increments of 10 min, and calculated the correlation value of the best-fitting cosine curve for each probe set. We selected the probe sets with correlation values above the cut off value of 0.8. To avoid noise and trivial oscillations, we extracted genes oscillating with high amplitude: we calculated the coefficient of variation of the six expression values, defined as its SD divided by the average expression value and selected the probe sets the coefficients of variations of which were above the cutoff value of 0.20. The peak-to-trough ratio was calculated for each probe set, and expressed as fold change (FC), in supplemental Table 1.

Expression data and other pertinent biological information have been deposited in the Gene Expression Omnibus (GEO) database (http://www.ncbi.nlm.nih.gov/geo/) with accession number: GSE2703. (ID: lemosd_rev_1; password: 720865595).

Hierarchical Clustering and Peak Time Analysis

Hierarchical clustering was performed on the 322 rhythmically expressed genes. Using average-linked cluster analysis, distances were measured by the cosine correlation coefficient for similarity measurement. To estimate the peak time of each gene, we estimated the peak time of each cycling gene from the peak time of the most highly correlated cosine wave. The transcripts were then clustered according to their peaking times.

sqRT-PCR

For experiment 1 (the 24-h profile study) and experiment 2 (the 100-h *vs.* 1300-h time point comparison study), 2 μg of total RNA was used for sqRT-PCR. The cDNA was synthesized using the Omniscript kit (QIAGEN) and oligo $d(T)_{15}$ primers (Promega Corp., Madison, WI). The reaction was performed following the manufacturer's instructions, in a 20-μl volume and at 37 C for 1 h. PCR amplifications were performed using 1 μl of cDNA, 200 μM deoxynucleotide triphosphates (Promega), 0.5 μM of each primer, and 2.5 U of HotStarTaq polymerase (QIAGEN) in 25 μl reaction. The reactions were performed using the following program: 95 C, 15 min; 94 C, 1 min; specific annealing temperature for each primer set, 1 min and 72 C, 1 min. Potential primers sequences were chosen using regions conserved in humans and mice. Those sequences were then Blasted against the monkey sequences available at the Human Genome Sequencing Center at Baylor College of Medicine (http://www.hgsc.bcm.tmc.edu/projects/rmacaque/), to obtain, whenever available, the monkey sequences. The primers were purchased from Invitrogen (Carlsbad, CA). The sequences were: Per1-F (forward), GCCAGCATCACTCGCAGCAGC; Per1-R (reverse), GTGGGTCATCAGGGTGACCAGG; Bmal1-F, CACAGCATGGACAGCATGCTGC; Bma1-R, GCCACCCAGTCCAGCATCTGC; Per2-F, CATCCACTGGTGGACCTCGCG; Per2-R, GGCTCACTGGGCTGCGACGC; Cry1-F, GCCTGTCCTAAGAGGCTTCCCTG; Cry1-R, ACTGAGACCAGTGCCCATGGAGC; PNMT-F, GGAGCATGTACAGCCAACATGCC; PNMT-R, CAGGCATGATATAGGTGCGGAGG; Slc6A2-F, GGAGAGCTACCAACTCTTGCCAG; Slc6A2-R, ACCCAGCTAGTCAGCTGCAGAC; Cyp11A1-F, GCCATCTATGCTCTGGGCCGAG; Cyp11A1-R, CCATCCTCTCTGATCACTGCTGG; Cyp17A1-F, GAGTGGCACCAGCCGGATCAG; Cyp17A1-R, CTCCAGGCCTGGCGCACCTTG; Rnp24-F, CCGTCCTAATGGCAGAGCTCTC; Rnp24-R, AAGCCACCACTCACTGGGACAC; Rpl13a-F, GCAGTCCAGGTGCCACAGGCAG; Rpl13a-R, AGGTGAGGAGCATGGGCGAT GC; β-actin-F, CATTGCTCCTCCTGAGCGCAAG; β-actin-R, GGGCCGGACTCGTCATACTCC. The number of PCR cycles was established after testing a range of 20–35 to ensure that the amount of DNA product remained in the logarithmic range of the amplification curve. Control reactions using the RNA samples were performed so as to rule out genomic contamination. PCR products (7 μl) were separated on 2% agarose gels, stained with ethidium bromide using electrophoresis, and were photographed under UV light.

Taqman Quantitative RT-PCR

The RNA was diluted to 0.1 μg/μl, and cDNA was prepared by random-primed reverse transcription using random hexamer primers (Promega), 200 ng of RNA, and the Omniscritp kit (QIAGEN). The reverse transcription reaction was diluted 1:100 for PCR analysis. The PCR mixtures contained 5 μl of Taqman Universal PCR Master Mix, 300 nM specific target gene primers, 50 nM human β-actin primers (Applied Biosystems, Foster City, CA), 250 nM specific probes, and 2 μl cDNA. Reactions were conducted in triplicate for higher accuracy. The amplification was performed as follows: 2 min at 50 C, 10 min at 95 C, and then 40 cycles each at 95 C for 15 sec and 60 C for 60 sec in an ABI/ Prism 7700 Sequences Detector System (Applied Biosystems). After completion of the PCR, baseline and threshold values were set to optimize the amplification plot. Standard curves were drawn on the basis of the log of the input RNA *vs.* the critical threshold cycle, which is the cycle during which the fluorescence of the sample was greater than the threshold of baseline fluorescence. Standard curves were used to convert the critical threshold values into relative RNA concentrations for each sample. The primers and probes were designed using PrimerExpress software (Applied Biosystems) and were purchased from Invitrogen and Sigma Genosys (St. Louis, MO), respectively. For Rev-erbα, the primers and probe were designed using the rhesus macaque sequence available in the GenBank database (accession no. BV208705); for TH, the human sequence was used (accession no. NM_199292). The sequences were: Rev-erbα-F, ACCCTGAACAACATGCATTCC; Rev-erbα-R, GGAGAGAGAAGTGCAGAGTTCGA, Rev-erbα probe, 5′-6FAM-CTGCCGCTGCCCCCTTGTACA-TAMRA-3′; TH-F, TCATCACCTGGTCACCAAGTTC; TH-R, CGATCTCAGCAATCAGCTTCCT; TH probe, 5′-6FAM-CTCGGACCAGGTGTACCGCCA-TAMRA-3′.

Immunohistochemistry

Right adrenal glands from experiment 1 (the 24-h profile study) were fixed in 4% paraformaldehyde, and 25-μm sections were cut using a frozen-stage sliding microtome; they were immediately transferred to a cryoprotectant solution and stored at −20 C until use. Single-label immunohistochemistry for REV-ERBα was performed as follows: floating tissue sections were removed from the cryoprotectant and washed in 0.02 M potassium PBS (KPBS). Antigen retrieval was performed by heating the tissue in 20 mM sodium citrate buffer, pH 9.0, in a water bath at 90 C, for 30 min. The sections were incubated in blocking buffer (KPBS + 0.5% Triton X-100 + 2% normal donkey serum) for 30 min, to reduce background staining, and then incubated in rabbit polyclonal human REV-ERBα antibody (1:1000; Lifespan Biosciences, Seattle, WA) for 48 h at 4 C. After washing in KPBS, the sections were incubated for 1 h in biotinylated donkey antirabbit antibody (1:500; Jackson ImmunoResearch Laboratories, Inc., West Grove, PA), washed, and then incubated in avidin-biotin solution (Vectastain, Vector Laboratories, Burlingame, CA) for 1 h. REV-ERBα -immunoreactivity was visualized using the chromagen 3,3′-diaminobenzidine tetrachloride (DAB) enhanced with nickel chloride. Double-label immunohistochemistry for REV-ERBα and TH was performed using the mouse polyclonal TH antibody. Briefly, after staining for REV-ERBα, the sections were incubated in mouse TH antibody (1:2000; Roche Clinical Laboratories, Indianapolis, IN) 24 h at 4 C. After washes in KPBS, the sections were incubated for 1 h in biotinylated donkey antimouse antibody (1:500; Jackson ImmunoResearch Laboratories) and then washed and incubated in avidin-biotin solution for 1 h. TH immunoreactivity was visualized with DAB without nickel enhancement. Negative controls were performed in which the primary antibodies were omitted. Sections from all of the experiments were mounted onto glass microscope slides and coverslipped.

Acknowledgments

We thank Dr. Claudio Mastronardi for his invaluable comments on the manuscript.

Received September 6, 2005. Accepted January 19, 2006.

Address all correspondence and requests for reprints to: Henryk F. Urbanski, Division of Neuroscience, Oregon National Primate Research Center, 505 Northwest 185th Avenue, Beaverton, Oregon 97006. E-mail: urbanski@ohsu.edu.

This work was supported by National Institutes of Health Grants AG-19914, AG-23477, DK-61766, HD-29186, and RR-00163. D.R.L. was supported by the Fogarty International Training Grant TW/HD-00668.

Author Disclosure Summary: D.R.L., H.F.U., and J.L.D. have nothing to declare.

REFERENCES

1. Campbell IT, Walker RF, Riad-Fahmy D, Wilson DW, Griffiths K 1982 Circadian rhythms of testosterone and cortisol in saliva: effects of activity-phase shifts and continuous daylight. Chronobiologia 9:389–396
2. Zhao ZY, Xie Y, Fu YR, Li YY, Bogdan A, Touitou Y 2003 Circadian rhythm characteristics of serum cortisol and dehydroepiandrosterone sulfate in healthy Chinese men aged 30 to 60 years. A cross-sectional study. Steroids 68:133–138
3. Hansen AM, Garde AH, Skovgaard LT, Christensen JM 2001 Seasonal and biological variation of urinary epinephrine, norepinephrine, and cortisol in healthy women. Clin Chim Acta 309:25–35
4. Bondanelli M, Ambrosio MR, Franceschetti P, Margutti A, Trasforini G, Degli Uberti EC 1999 Diurnal rhythm of plasma catecholamines in acromegaly. J Clin Endocrinol Metab 84:2458–2467
5. Urbanski HF, Downs JL, Garyfallou VT, Mattison JA, Lane MA, Roth GS, Ingram DK 2004 Effect of caloric restriction on the 24-hour plasma DHEAS and cortisol profiles of young and old male rhesus macaques. Ann NY Acad Sci 1019:443–447
6. Moore RY, Eichler VB 1972 Loss of a circadian adrenal corticosterone rhythm following suprachiasmatic lesions in the rat. Brain Res 42:201–206
7. Meyer-Bernstein EL, Jetton AE, Matsumoto SI, Markuns JF, Lehman MN, Bittman EL 999 Effects of suprachiasmatic transplants on circadian rhythms of euroendocrine function in golden hamsters. Endocrinology 140:207–218
8. Buijs RM, Wortel J, Van Heerikhuize JJ, Feenstra MG, Ter Horst GJ, Romijn HJ, Kalsbeek A 1999 Anatomical and functional demonstration of a multisyntaptic suprachiasmatic nucleus adrenal (cortex) pathway. Eur J Neurosci 11:1535–1544
9. Kalsbeek A, Ruiter M, la Fleur SE, Van Heijningen C, Buijs RM 2003 The diurnal modulation of hormonal responses in the rat varies with different stimuli. J Neuroendocrinol 15:1144–1155
10. Balsalobre A 2002 Clock genes in mammalian peripheral tissues. Cell Tissue Res 309:193–199
11. Balsalobre A, Damiola F, Schibler U 1998 A serum shock induces circadian gene expression in mammalian tissue culture cells. Cell 93:929–937
12. Yamazaki S, Numano R, Abe M, Hida A, Takahashi R, Ueda M, Block GD, Sakaki Y, Menaker M, Tei H 2000 Resetting central and peripheral oscillators in transgenic rats. Science 288:682–685
13. McNamara P, Seo S, Rudic RD, Sehgal A, Chakravarti D, FitzGerald GA 2001 Regulation of clock and mop4 by nuclear hormone receptors in the vasculature. A humoral mechanism to reset a peripheral clock. Cell 105:877–889
14. Reppert SM, Weaver DR 2002 Coordination of circadian timing in mammals. Nature 418:935–941
15. Okamura, H 2004 Clock genes in cell clocks: roles, actions, and mysteries. J Biol Rhythms 19:388–399
16. Reppert SM, Weaver DR 2001 Molecular analysis of mammalian circadian rhythms. Annu Rev Physiol 63: 647–676
17. Kume K, Zylka MJ, Sriram S, Shearman LP, Weaver DR, Jin X, Maywood ES, Hastings MH, Reppert SM 1999 mCRY1 and mCRY2 are essential components of the negative limb of the circadian clock feedback loop. Cell 98:193–205
18. Yagita k, Yamaguchi S, Tamanini F, van Der Horst GT, Hoeijmakers JH, Yasui A, Loros JJ, Dunlap JC, Okamura H 2000 Dimerization and nuclear entry of mPER proteins in mammalian cells. Genes Dev 14:1353–1363
19. Storch KF, Lipan O, Leykin I, Viswanathan N, Davis FC, Wong WH, Weitz CJ 2002 Extensive and divergent circadian gene expression in liver and heart. Nature 417:78–83
20. Panda S, Antoch MP, Miller BH, Su AI, Schook AB, Straume M, Schultz PG, Kay SA, Takahashi JS, Hogenesch JB 2002 Coordinated transcription of key pathways in the mouse by the circadian clock. Cell 109:307–320
21. Akhtar RA, Reddy AB, Maywood ES, Clayton JD, King VM, Smith AG, Gant TG, Hastings MH, Kyriacou CP 2002 Circadian cycling of the mouse liver transcriptome, as revealed by cDNA microarray, is driven by the suprachiasmatic nucleus. Curr Biol 12:540–550
22. Ueda HR, Chen W, Adachi A, Wakamatsu H, Hayashi S, Takasugi T, Nagano M, Nakahama K, Suzuki Y, Sugano S, Iino M, Shigeyoshi Y, Hashimoto S 2002 A transcription factor response element for gene expression during circadian night. Nature 418:534–539
23. Gorbacheva VY, Kondratov RV, Zhang R, Cherukuri S, Gudkov A, Takahashi JS, Antoch MP 2005 Circadian sensitivity to the chemoterapeutic agent cyclophosphamide depends on the functional status of the CLOCK/BMAL1 transactivation complex. Proc Natl Acad Sci USA 9:3407–3412
24. Hastings MH, Reddy AB, Maywood ES 2003 A clockwork web: circadian timing in brain and periphery, in health and disease. Nat Rev Neurosci 4:649–661
25. Bjarnason GA, Jordan RC, Wood PA, Li Q, Lincoln DW, Sothern RB, Hrushesky WJ, Ben-David Y 2001 Circadian expression of clock genes in human oral mucosa and skin: association with specific cell-cycle phases. Am J Pathol 158:1793–1801
26. Zambon AC, McDearmon EL, Salomonis N, Vranizan KM, Johansen KL, Adey D, Takahashi JS, Schambelan M, Conklin BR 2003 Time- and exercise-dependent gene regulation in human skeletal muscle. Genome Biol 4(10):R61
27. Brown SA, Fleury-Olela F, Nagoshi E, Hauser C, Juge C, Meier CA, Chicheportiche R, Dayer JM, Albrecht U, Schibler U 2005 The period length of fibroblast circadian gene expression varies widely among human individuals. PLoS Biol 3:1813–1818
28. Bittman EL, Doherty L, Huang L, Paroskie A 2003 Period gene expression in mouse endocrine tissues. Am J Physiol Regul Integr Comp Physiol 285:561–569
29. Ishida A, Mutoh T, Ueyama T, Bando H, Masubuchi S, Nakahara D, Tsujimoto G, Okamura H 2005 Light activates the adrenal gland: timing of gene expression and glucocorticoid release. Cell Metab 2:297–307
30. Wilson MM, Rice RW, Critchlow V 1976 Evidence for a free-running circadian rhythm in pituitary-adrenal function in blinded adult female rats. Neuroendocrinology 20:289–295
31. Takahashi K, Inoue K, Takahashi Y 1977 Parallel shift in circadian rhythms of adrenocortical activity and food intake in blinded and intact rats exposed to continuous illumination. Endocrinology 100:1097–1107
32. Swan C, Abe K, Critchlow V 1978 Effects of age of blinding on rhythmic pituitary-adrenal function in female rats. Neuroendocrinology 27:175–185
33. Bornstein SR, Ehrhart-Bornstein M, Scherbaum WA, Pfeiffer EF, Holst JJ 1990 Effects of splanchnic nerve stimulation on the adrenal cortex may be mediated by chromaffin cells in a paracrine manner. Endocrinology 127:900–906
34. Bornstein SR, Ehrhart-Bornstein M, Usadel H, Bockmann M, Scherbaum WA 1991 Morphological evidence

for a close interaction of chromaffin cells with cortical cells within the adrenal gland. Cell Tissue Res 265:1–9
35. Shepherd SP, Holzwarth MA 2001 Chromaffin-adrenocortical cell interactions: effects of chromaffin cell activation in adrenal cell cocultures. Am J Physiol Cell Physiol 280:C61–C71
36. Bartness TJ, Song CK, Demas GE 2001 SCN efferents to peripheral tissues: implications for biological rhythms. J Biol Rhythms 16:196–204
37. Jasper MS, Engeland WC 1994 Splanchnic neural activity modulates ultradian and circadian rhythms in adrenocortical secretion in awake rats. Neuroendocrinology 59: 97–109
38. Sewer MB, Waterman MR 2003 ACTH modulation of transcription factors responsible for steroid hydroxylase gene expression in the adrenal cortex. Microsc Res Tech 61:300–307
39. Parker CR Jr., Stankovic AK, Faye-Petersen O, Falany CN, Li H, Jian M 1998 Effects of ACTH and cytokines on dehydroepiandrosterone sulfotransferase messenger RNA in human adrenal cells. Endocr Res 24:669–673
40. Allen-Rowlands CF, Allen JP, Greer MA, Wilson M 1980 Circadian rhythmicity of ACTH and corticosterone in the rat. J Endocrinol Invest 3:371–377
41. John ME, John MC, Boggaram V, Simpson ER, Waterman MR 1986 Transcriptional regulation of steroid hydroxylase genes by corticotropin. Proc Natl Acad Sci USA 83:4715–4719
42. Guse-Behling H, Ehrhart-Bornstein M, Bornstein SR, Waterman MR, Scherbaum WA, Adler G 1992 Regulation of adrenal steroidogenesis by adrenaline: expression of cytochrome P450 genes. J Endocrinol 135:229–237
43. Noshiro M, Kawamoto T, Furukawa M, Fujimoto K, Yoshida Y, Sasabe E, Tsutsumi S, Hamada T, Honma S, Honma K, Kato Y 2004 Rhythmic expression of DEC1 and DEC2 in peripheral tissues: DEC2 is a potent suppressor for hepatic cytochrome P450s opposing DBP. Genes Cells 9:317–329
44. Akiyama T, Yamazaki T, Mori H, Sunagawa K 2003 Inhibition of cholinesterase elicits muscarinic receptor-mediated synaptic transmission in the rat adrenal medulla. Auton Neurosci 107:65–73
45. Yoon SO, Chikaraishi DM 1994 Isolation of two E-box binding factors that interact with the rat tyrosine hydroxylase enhancer. J Biol Chem 269:18453–18462
46. Kim CH, Ardayfio P, Kim KS 2001 An E-box motif residing in the exon/intron 1 junction regulates both transcriptional activation and splicing of the human norepinephrine transporter gene. J Biol Chem 276:24797–24805
47. Nicolau GY 1974 Rhythmic circadian variations of RNA concentration in the rabbit adrenal. Rev Roum Med 12: 333–337
48. Nicolau GY 1979 Persistence of circadian rhythms of RNA, DNA and protein in the rat adrenal and thyroid under continuous darkness conditions. Endocrinologie 17:177–183
49. McDonald MJ, Rosbash M 2001 Microarray analysis and organization of circadian gene expression in *Drosophila*. Cell 107:567–578
50. Harmer SL, Hogenesch JB, Straume M, Chang H-S, Han B, Zhu T, Wang X, Kreps JA, Kay SA 2000 Orchestrated transcription of key pathways in *Arabidopsis* by the circadian clock. Science 290:2110–2113
51. Duffield GE, Best JD, Meurers BH, Bitner A, Loros JJ, Dunlap JC 2002 Circadian programs of transcriptional activation, signaling, and protein turnover revealed by microarray analysis of mammalian cells. Curr Biol 12:551–557
52. Ueda HR, Chen W, Minami Y, Honma S, Honma K, Iino M, Hashimoto S 2004 Molecular-timetable methods for detection of body time and rhythm disorders from single-time-point genome-wide expression profiles. Proc Natl Acad Sci USA 101:11227–11232
53. Kato H, Saito M, Suda M 1980 Effect of starvation on the circadian adrenocortical rhythm in rats. Endocrinology 106:918–921
54. Szafarczyk A, Ixart G, Alonso G, Malaval F, Nouguier-Soule J, Assenmacher I 1983 CNS control of the circadian adrenocortical rhythm. J Steroid Biochem 19:1009–1015
55. Banky Z, Halasz B, Nagy G 1986 Circadian corticosterone rhythm did not develop in rats seven weeks after destruction with 5,7-dihydroxytryptamine of the serotoninergic nerve terminals in the suprachiasmatic nucleus at the age of 16 days. Brain Res 369:119–124
56. Andrews RV, Folk Jr GE 1964 Circadian metabolic patterns in cultured hamster adrenal glands. Comp Biochem Physiol 11:393–409
57. Andrews RV 1968 Daily variation in membrane flux of cultured hamster adrenals. Comp Biochem Physiol 26: 479–488
58. Andrews RV 1971 Circadian rhythms in adrenal organ cultures. Gegenbaurs Morphol Jahrb 117:89–98
59. Shearman LP, Sriram S, Weaver DR, Maywood ES, Chaves I, Zheng B, Kume K, Lee CC, van der Horst GT, Hastings MH 2000 Interactin molecular loops in the mammalian circadian clock. Science 288:1013–1019
60. Albrecht U, Zheng B, Larkin D, Sun ZS, Lee CC 2001 MPer1 and mper2 are essential for normal resetting of the circadian clock. J Biol Rhythms 16:100–104
61. Ghizzoni L, Mastorakos, G 2003 Interactions of leptin, GH, and cortisol in normal children. Ann NY Acad Sci 997:56–63
62. Mancini T, Kola B, Mantero F, Boscaro M, Arnaldi G 2004 High cardiovascular risk in patients with Cushing's syndrome according to 1999 WHO/ISH guidelines. Clin Endocrinol (Oxf) 61:768–777
63. Bravo EL 2002 Pheochromocytoma. Cardiol Rev 1:44–50
64. Bethea CL, Streicher JM, Mirkes SJ, Sanchez RL, Reddy AP, Cameron JL 2005 Serotonin-related gene expression in female monkeys with individual sensitivity to stress. Neuroscience 132:151–166
65. Lane MA, Ingram DK, Ball SS, Roth GS 1997 Dehydroepiandrosterone sulfate: a biomarker of primate aging slowed by calorie restriction. J Clin Endocrinol Metab 82:2093–2096
66. Roth GS, Mattison JA, Ottinger MA, Chachich ME, Lane MA, Ingram DK 2004 Aging in rhesus monkeys: relevance to human health interventions. Science 305: 1423–1426
67. Kayo T, Allison DB, Weindruch R, Prolla TA 2001 Influences of aging and caloric restriction on the transcriptional profile of skeletal muscle from rhesus monkeys. Proc Natl Acad Sci USA 9:5093–5098
68. Wang Z, Lewis MG, Nau ME, Arnold A, Vahey MT 2004 Identification and utilization of inter-species conserved probe sets on Affymetrix human GeneChip platforms for the optimization of the assessment of expression patterns in nonhuman primate (NHP) samples. BMC Bioinformatics 5:165

Molecular Endocrinology **is published monthly by The Endocrine Society (http://www.endo-society.org), the foremost professional society serving the endocrine community.**